
# Incorporating Anthropogenic Water Regulation Modules into a Land Surface Model

YADU POKHREL,* NAOTA HANASAKI,+ SUJAN KOIRALA,# JAEIL CHO,@ PAT J.-F. YEH,*
HYUNGJUN KIM,&,* SHINJIRO KANAE,# AND TAIKAN OKI*

* *Institute of Industrial Science, University of Tokyo, Tokyo, Japan*
+ *National Institute for Environmental Studies, Tsukuba, Japan*
# *Department of Mechanical and Environmental Informatics, Tokyo Institute of Technology, Tokyo, Japan*
@ *Kasuya Research Forest, Kyushu University, Fukuoka, Japan*
& *Center for Hydrologic Modeling, University of California, Irvine, Irvine, California*

(Manuscript received 2 February 2011, in final form 13 July 2011)

ABSTRACT

Anthropogenic activities have been significantly perturbing global freshwater flows and groundwater reserves. Despite numerous advances in the development of land surface models (LSMs) and global terrestrial hydrological models (GHMs), relatively few studies have attempted to simulate the impacts of anthropogenic activities on the terrestrial water cycle using the framework of LSMs. From the comparison of simulated terrestrial water storage with the Gravity Recovery and Climate Experiment (GRACE) satellite observations it is found that a process-based LSM, the Minimal Advanced Treatments of Surface Interaction and Runoff (MATSIRO), outperforms the bucket-model-based GHM called H08 in simulating hydrologic variables, particularly in water-limited regions. Therefore, the water regulation modules of H08 are incorporated into MATSIRO. Further, a new irrigation scheme based on the soil moisture deficit is developed. Incorporation of anthropogenic water regulation modules significantly improves river discharge simulation in the heavily regulated global river basins. Simulated irrigation water withdrawal for the year 2000 (2462 $km^3\ yr^{-1}$) agrees well with the estimates provided by the Food and Agriculture Organization (FAO). Results indicate that irrigation changes surface energy balance, causing a maximum increase of ~50 $W\ m^{-2}$ in latent heat flux averaged over June–August. Moreover, unsustainable anthropogenic water use in 2000 is estimated to be ~450 $km^3\ yr^{-1}$, which corresponds well with documented records of groundwater overdraft, representing an encouraging improvement over the previous modeling studies. Globally, unsustainable water use accounts for ~40% of blue water used for irrigation. The representation of anthropogenic activities in MATSIRO makes the model a suitable tool for assessing potential anthropogenic impacts on global water resources and hydrology.

## 1. Introduction

Even though abundant water is available on the earth and its amount and circulation will not diminish on shorter-than-geological time scales, only a tiny fraction of it is freshwater and an even smaller fraction is easily accessible to humans (Oki and Kanae 2006). The growing human population and associated water use have been greatly perturbing the freshwater flows globally (Vörösmarty et al. 2000; Nilsson et al. 2005; Hanasaki et al. 2006). According to Vörösmarty and Sahagian (2000), global water withdrawal is approximated as 4000–5000 $km^3\ yr^{-1}$—about 10%–15% of long-term mean annual runoff volume (Oki and Kanae 2006). Despite being relatively smaller than the total renewable freshwater resources available in the world, human water use has significantly altered natural flow regimes and depleted groundwater reserves over the last century (Haddeland et al. 2006a; Döll et al. 2009; Rodell et al. 2009; Wada et al. 2010), posing an alarming threat to human water security and the well-being of aquatic ecosystems (Vörösmarty et al. 2010).

Water withdrawal for irrigation, which is the largest portion of human water extractions, represents ~70% of total water withdrawals and ~90% of consumptive water use (Shiklomanov and Rodda 2003; Rost et al. 2008). The demand for irrigation water use is still rising since agriculture is the major driver of economic development in many developing countries (Cśaki and de Haan 2003) where the expansion of croplands or extension of irrigation facilities is inevitable to feed the burgeoning population in the coming decades (Shiklomanov 2000). Water used

*Corresponding author address:* Yadu Pokhrel, Institute of Industrial Science, 4-6-1 Meguro, Komaba, Tokyo 153-8505, Japan.
E-mail: pokhrel@rainbow.iis.u-tokyo.ac.jp

DOI: 10.1175/JHM-D-11-013.1

for irrigation returns to the atmosphere through evapotranspiration or back to rivers as return flow, which can potentially affect the terrestrial water and energy balances (Haddeland et al. 2006b; Tang et al. 2007; Ozdogan et al. 2010) as well as the flow of water vapor into the atmosphere (Boucher et al. 2004; Sacks et al. 2009; Puma and Cook 2010). Such increase in agricultural water demand is likely to raise the pressure on water resources, particularly in regions where water is no longer abundant (Cai and Rosegrant 2002). These concerns about water resources have drawn considerable attention from hydrology and climate research communities in emphasizing the urgent need for developing integrated water resources models to simulate the impact of anthropogenic activities on the terrestrial water cycle.

In recent years, a number of macroscale hydrological models have been developed to assess anthropogenic disturbance on global water resources (e.g., Alcamo et al. 2003; Haddeland et al. 2006a,b; Wisser et al. 2010a; Rost et al. 2008; Hanasaki et al. 2008a,b). Although these models have been successfully applied to global-scale water resources assessments, the majority of them have been developed in an offline mode without coupling with the general circulation models (GCMs). In most of these global terrestrial hydrological models (GHMs) (see a comprehensive overview by Haddeland et al. 2011), land surface hydrologic processes are often treated in a rather conceptual way and surface energy balance critical to the evaporation process is not considered. In contrast, the land surface models (LSMs) used for climate modeling studies solve both water and energy balances. Since land surface hydrological processes exert profound influence on the overlying atmosphere (Shukla and Mintz 1982; Koster et al. 2004), LSMs have been advanced through intensive improvements in many aspects of model parameterizations from both the atmospheric and hydrologic communities (Sellers et al. 1997). However, few of these efforts have addressed the issue of human impacts on the terrestrial water cycle by explicitly representing them within the framework of LSMs.

De Rosnay et al. (2003) integrated an irrigation scheme into the LSM Organizing Carbon and Hydrology in Dynamic Ecosystems (ORCHIDEE; Ducoudré et al. 1993) to assess the impact of irrigation on the Indian peninsula. They successfully simulated irrigation water requirements and showed that intensive irrigation has a regional impact on the partitioning of energy between sensible and latent heat fluxes. However, they did not consider the effect of reservoir operation on the temporal variability of water available in the river channels. Several other modeling studies have quantified the influence of irrigation on regional climate (Boucher et al. 2004; Lobell et al. 2009; Sacks et al. 2009; Puma and Cook 2010). In these studies, the volume of annual irrigation water was commonly fixed at a mean value based on earlier reports (e.g., Döll and Siebert 2002; Helkowski 2004), or soil moisture in irrigated areas was set to the saturation throughout the year, independent of crop cycle. Therefore, the temporal dynamics of irrigation water requirement was largely ignored. In reality, however, irrigation water requirement varies both spatially and temporally and is significantly affected by the local hydrometeorological conditions (Döll and Siebert 2002).

Hanasaki et al. (2008a,b) developed the integrated water resources assessment model H08 to simulate both natural and anthropogenic flows of water globally. However, H08 is based on a simple bucket model (Manabe 1969; Robock et al. 1995) modified for the subsurface runoff generation by adding an outlet to the bucket, commonly known as the leaky bucket. The model consists of only one soil layer of 1-m depth and vegetation processes are accounted in an implicit way by using a globally uniform bulk transfer coefficient of 0.003. Therefore, global water resources assessment using H08 to some extent compromises the realistic representation of land surface hydrology.

In this study, we incorporate the anthropogenic water regulation modules derived from the H08 model into a process-based LSM, namely the Minimal Advanced Treatments of Surface Interaction and Runoff (MATSIRO; Takata et al. 2003). In addition, a new irrigation scheme based on the soil moisture deficit is developed and incorporated into the MATSIRO model. Our research objectives in this study are twofold. The first objective is to develop an integrated modeling framework for assessing the impact of anthropogenic water regulation on the terrestrial water cycle. The developed modeling framework is ready to be coupled to GCMs for studying the potential climate impacts and feedbacks. The second objective is to investigate the applicability of a newly developed irrigation scheme for use in advanced LSMs. This paper describes the development, evaluation, and an application of the integrated model.

The data used in this modeling study and the development of the integrated model are described in sections 2 and 3, respectively. Section 4 presents model evaluation and the analysis of irrigation-induced changes on surface energy balance. In section 5, an application of the integrated model in simulating water withdrawals from different sources is demonstrated. Finally, summary and conclusions are presented in section 6.

## 2. Data

### *a. Climate data*

The spatial resolution of forcing data and simulations is $1^\circ \times 1^\circ$ (longitude and latitude) global grids with

a land–sea mask defined by the Global Soil Wetness Project 2 (GSWP2; Dirmeyer et al. 2006). Atmospheric forcing data covering the 29-yr simulation period (1979–2007) are obtained from Kim et al. (2009). The data include 6-hourly precipitation, temperature, radiations, surface pressure, specific humidity, and wind speed based on the atmospheric reanalysis data provided by the Japanese Meteorological Agency (JMA) Climate Data Assimilation System (JCDAS; Onogi et al. 2007). An altitude correction (Ngo-Duc et al. 2005) is applied to temperature, pressure, and humidity and all variables are bilinearly interpolated into the $1° \times 1°$ grids. The 6-hourly reanalysis precipitation fields are used to temporally disaggregate the observed monthly or daily precipitation data. Kim et al. (2009) produced five different observation-based 6-hourly precipitation data at $1° \times 1°$ grids by bilinearly interpolating or aggregating from their original spatial resolution. For the baseline simulation, we use the Global Precipitation Climatology Center (GPCC; Rudolf and Schneider 2005) based precipitation data. The other four precipitation datasets—Global Precipitation Climatology Project (GPCP) version 2 (Adler et al. 2003), Climate Prediction Center (CPC) unified (Chen et al. 2008), Precipitation Reconstruction over Land (PREC/L; Chen et al. 2002), and CPC Merged Analysis of Precipitation (CMAP; Xie and Arkin 1997)—are used to examine the uncertainty in global irrigation water requirements caused by the precipitation data used. All results are based on GPCC precipitation data unless otherwise specified.

### b. Land cover, soil, LAI, and agricultural data

Current land cover, soil texture, and soil and vegetation parameters are taken from the GSWP2 (Dirmeyer et al. 2006). Monthly leaf area index (LAI) values are prescribed as same as in Hirabayashi et al. (2005). Data for irrigated areas around the year 2000 are obtained from the University of Frankfurt–Food and Agriculture Organization (FAO) Global Map of Irrigation Areas (GMIA) (Siebert et al. 2007). The original data, consisting of irrigated areas within a grid cell of 5 arc minutes, are spatially aggregated to $1° \times 1°$ grids using the GSWP2 land–sea mask. Time series of irrigated areas are obtained by extrapolating the GMIA data backward and forward over the entire simulation period, based on the national-level historical extent of irrigated areas provided by the University of Frankfurt (Freydank and Siebert 2008). Country-specific scaling factors are obtained for each year and the national total irrigated areas are distributed within the country following the distribution of the GMIA data. Irrigated areas are constrained within croplands using the historical evolution of cropland areas (Ramankutty and Foley 1999). For the period of 2004–07, the extent of irrigated areas is assumed to be as the same as that in 2003 because the data of Freydank and Siebert (2008) are available only until 2003.

### c. Reservoir data

Reservoir data are taken from Hanasaki et al. (2006) in which in total 498 reservoirs with the maximum storage capacity larger than $1 \times 10^9$ m$^3$ were located on the digital river network map (Oki and Sud 1998) based on the information provided by the *World Register of Dams 1998* (ICOLD 1998). Here, we update this database by adding ~50 new reservoirs with the maximum storage capacity larger than $1 \times 10^9$ m$^3$ based on the updated information from the *World Register of Dams 2003* (ICOLD 2003). The combined storage capacity of the updated reservoir database is 4680 km$^3$, which accounts for ~67% of the total storage capacity of all dams with a height of more than 15 m (ICOLD 1998). Additionally, the data for medium-sized reservoirs, representing small ponds with the storage capacity ranging from $3 \times 10^6$ to $1 \times 10^9$ m$^3$, are also obtained from Hanasaki et al. (2010). These medium-sized reservoirs are distributed spatially in proportion to the population distribution considering the total national storage capacity.

## 3. Model description and design of simulations

### a. The MATSIRO LSM and river routing model TRIP

The core of the integrated modeling framework is the process-based LSM MATSIRO (Takata et al. 2003), developed to compute the hydrological and biophysical exchanges in a GCM, namely the Model for Interdisciplinary Research on Climate (MIROC) (Hasumi and Emori 2004). MATSIRO simulates the exchange of water vapor, energy, and momentum between the land surface and atmosphere on a physical basis. Effects of vegetation on surface energy balance are calculated by a multilayer canopy model (Watanabe 1994) and a photosynthesis–stomatal conductance model (Collatz et al. 1991). A simplified TOPMODEL (Beven and Kirkby 1979; Stieglitz et al. 1997) is used to represent surface and subsurface runoff processes, and river routing is accounted by integrating the river routing model Total Runoff Integrating Pathways (TRIP) (Oki and Sud 1998) into the LSM.

### b. Incorporating anthropogenic water regulation modules into MATSIRO

Four different anthropogenic water regulation modules (crop growth module, reservoir operation module, water withdrawal module, and environmental flow requirement module) derived from H08 (Hanasaki et al. 2008a,b) are incorporated into the MATSIRO–TRIP

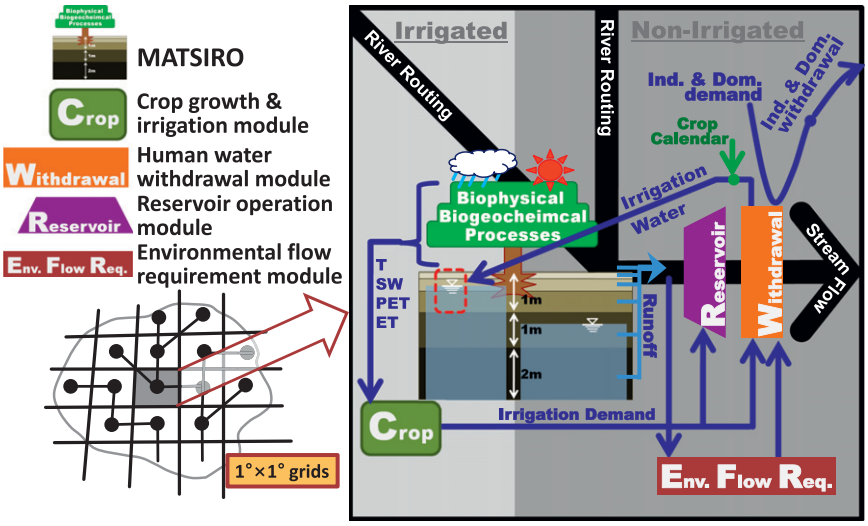


FIG. 1. Schematic diagram of the integrated modeling framework. Here $T$, SW, PET, and ET denote air temperature, shortwave radiation, potential evapotranspiration, and evapotranspiration, respectively.

modeling framework. Figure 1 shows a schematic diagram of the integrated model. In the fully integrated mode, the runoff output of MATSIRO is routed through the digital river network of TRIP using the optimal constant flow velocity of 0.5 m $s^{-1}$ as suggested by some previous global-scale modeling studies (e.g., Oki et al. 1999; Decharme et al. 2010). TRIP routes both surface and subsurface runoff to the river mouth, implicitly taking into account the shallow groundwater movement that is not represented in MATSIRO. The operation module of reservoirs (located in the river network map) is activated for grid cells with a reservoir. The withdrawal module obtains domestic, industrial, and agricultural water from river channels considering the lower threshold of river discharge prescribed by the environmental flow requirement module. However, there is an option to withdraw water from the predefined local sources such as natural streams and medium-sized reservoirs; or unlimitedly once from an imaginary source if the local sources run out. This imaginary source is identical to the nonrenewable and nonlocal blue water (NNBW) suggested by Rost et al. (2008) to implicitly account for water withdrawal from nonrenewable fossil groundwater. The use of nonrenewable groundwater is usually considered unsustainable because nonrenewable water use over a prolonged period causes groundwater depletion (Wada et al. 2010). Although the imaginary source represents groundwater, it serves merely as an unlimited source of water and does not explicitly take into account the actual groundwater recharge. Finally, water remaining in the river channels flows downstream to the ocean or inland sinks. The following subsections provide brief descriptions of each module.

#### 1) CROP GROWTH MODULE AND THE IRRIGATION SCHEME

The crop growth module, which is based on crop vegetation formulations and parameters of the Soil and Water Integrated Model (SWIM; Krysanova et al. 1998), estimates the cropping period necessary to obtain mature and optimal total plant biomass for 18 different crop types (Leff et al. 2004). In the SWIM model more than 50 crop types are considered. In this study, the crop types of the SWIM model not included in the 18 crop types of Leff et al. (2004) are treated as generic crops. Double cropping is taken into account by assuming that the primary (secondary) crop is cultivated as the first (second) crop. In the double-cropping grid cells, the second crop is planted after the first is harvested. The primary and secondary crop type data are obtained from Leff et al. (2004). Irrigated areas for the first and second crops are estimated based on the data of cropping intensity (Döll and Siebert 2002). Subgrid variability of crops within irrigated areas is not considered in this study.

To estimate a crop calendar, the crop module requires downward shortwave radiation, air temperature, and the actual and potential evapotranspiration. The MATSIRO calculates evapotranspiration by solving energy balance at the soil and canopy surfaces; potential evapotranspiration is not estimated. Therefore, a potential evapotranspiration scheme based on the FAO Penman–Monteith method (Allen et al. 1998) is incorporated. To estimate daily potential evapotranspiration, mean daily air temperature, short wave radiation, wind speed, vapor

pressure, and ground heat flux are provided from the MATSIRO land surface driver.

Irrigation water demand is calculated from the soil moisture deficit in the root zone. MATSIRO has five soil layers with a total thickness of 4 m (0.05, 0.20, 0.75, 1.0, and 2.0 m from the land surface). The top 1 m (i.e., top three layers) is considered as the root zone for the calculation of irrigation demand. The soil moisture deficit for crops is defined as the difference in target soil moisture content (TSMC) and actual soil moisture content. Irrigation demand is calculated in each time step as,

$$I = \frac{\rho_w}{\Delta t} \sum_{k=1}^{3} \{\max[(\mathrm{TSMC} - \theta_k), 0] D_k\}, \qquad (1)$$

where $\mathrm{TSMC} = \alpha \times \theta_s$, $I$ (kg m$^{-2}$ s$^{-1}$) is the irrigation demand; $\rho_w$ (kg m$^{-3}$) is the density of water; $\Delta t$ is the model time step; $\theta_s$ and $\theta_k$ (m$^3$ m$^{-3}$) are the soil porosity and simulated actual soil moisture content, respectively; and $D_k$ (m) is the thickness of $k$th soil layer from the land surface. The $\alpha$ is set at 1 for rice and 0.75 for the other crops.

Each grid cell is divided into two independent tiles: nonirrigated and irrigated areas, respectively, to solve energy and water balances. Vegetation cover in the first and second tiles is set to potential vegetation and cropland, respectively, and the irrigation module is activated only in the second tile. Therefore, each tile independently tracks land surface states and fluxes for nonirrigated and irrigated conditions, respectively. For grid cells assigned to irrigated areas, the area-weighted averages are calculated using the fractional weights of nonirrigated and irrigated areas. The data of irrigated area fraction are obtained from Siebert et al. (2007). For the irrigated areas, the climatological LAI is updated with the growing season LAI simulated by the crop growth module. Thus, the irrigation scheme runs in a consistent manner within the LSM and also interacts with the crop growth module.

Irrigation water is applied to soil surface starting from 30 days prior to the planting date until crop harvest. Preplanting irrigation is applied to avoid a heavy irrigation requirement on the planting day (particularly in water-limited regions) by assuming a linear increase of soil moisture to TSMC on the planting date.

#### 2) Reservoir operation, water withdrawal, and environmental flow requirement modules

The reservoir operation, water withdrawal, and environmental flow requirement modules are incorporated into the river routing model. The reservoir operation module is identical to that of Hanasaki et al. (2006). The water withdrawal module withdraws the total water demand of a grid cell, estimated as the sum of agricultural, domestic, and industrial demands. Agricultural demand is simulated by the irrigation module, but domestic and industrial demands are not simulated. Therefore, we use the data of Hanasaki et al. (2008a), which are based on the FAO's AQUASTAT country statistics (FAO 2007). Water flowing through a grid cell is stored in the medium-sized reservoirs, which can be used later when water is not available in the river channels. Water diversion is not considered in this study; only the water flowing through the grid cell can be withdrawn, including the local runoff, accumulated runoff from the upstream grids, and water released from upstream reservoirs. The environmental flow requirement module is identical to that of Hanasaki et al. (2008b).

TABLE 1. Overview of simulation design.

| Simulation | Land[a] | River[b] | Crop/Irr.[c] | Res.[d] | Wit.[e] | Env.[f] |
|---|---|---|---|---|---|---|
| MAT-NAT | MATSIRO | ✓ | — | — | — | — |
| CRP-CAL | — | — | ✓ | — | — | — |
| MAT-IRG | MATSIRO | — | ✓ | — | — | — |
| MAT-HI | MATSIRO | ✓ | ✓ | ✓ | ✓ | ✓ |
| H08-NAT | Bucket | ✓ | — | — | — | — |
| H08 | Bucket | ✓ | ✓ | ✓ | ✓ | ✓ |

[a] Land surface hydrology model.
[b] River routing model TRIP.
[c] Crop growth and irrigation module.
[d] Reservoir operation module.
[e] Water withdrawal module.
[f] Environmental flow requirement module.

### c. *Integration and design of simulations*

The integrated model has the option to turn each water regulation module on and off. To run the model in a fully integrated mode, the following three simulations are necessary (Table 1). First, the natural simulation (MAT-NAT) is conducted by turning all human impact modules off to obtain the natural annual river discharge, potential evapotranspiration, and actual evapotranspiration. Second, the crop growth and irrigation modules are run in a standalone mode to estimate the crop calendar (CRP-CAL). For this simulation, climate data (air temperature and downward shortwave radiation) and the actual and potential evapotranspiration estimated from the MAT-NAT simulation are used as the input. Planting date, harvesting date, and growing season LAI for the first and second crops in each grid cell are obtained. Third, the LSM and irrigation module are coupled (MAT-IRG) to obtain the potential annual irrigation water requirement. Finally, all modules are activated and a fully integrated human impact (MAT-HI) run is conducted. The long-term mean annual river discharge and irrigation demand, obtained from the MAT-NAT and MAT-IRG simulations, respectively,

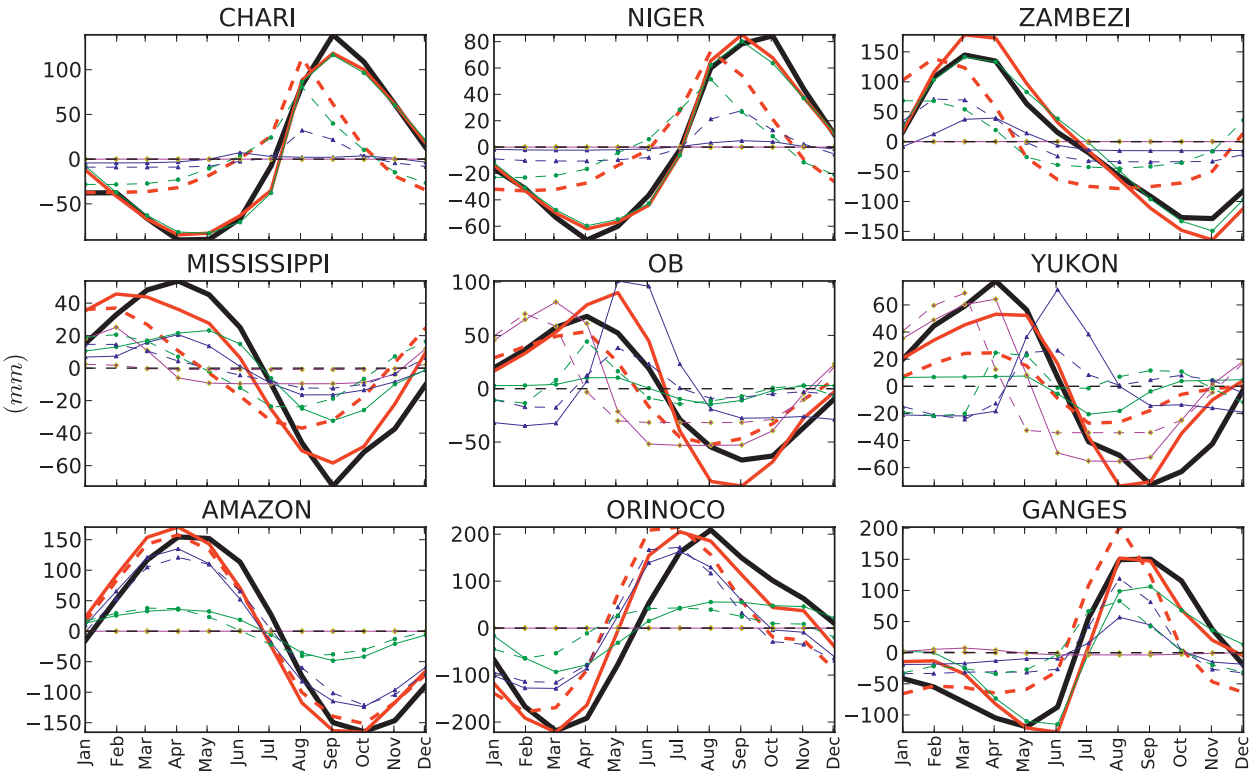


FIG. 2. Comparison of seasonal cycle of monthly TWSA from GRACE observations (black thick line) with simulated TSWA (red line) for 2002–07. Green, blue, and purple lines indicate soil moisture, river storage including shallow groundwater, and snow storage, respectively. For simulated TWSA, solid and dashed lines of same color indicate the MAT-NAT and H08-NAT simulations, respectively. All values are shown in mm.

are used in the reservoir operation module of the MAT-HI simulation to estimate the release of water from reservoirs.

As summarized in Table 1, a series of simulations is performed. After preparing all necessary input data, 29-yr (1979–2007) offline simulations are conducted with MAT-NAT and MAT-HI simulation designs (Table 1). The model runs at the hourly time step, while the output is daily. Identical forcing and initial conditions of hydrologic states are used for both simulations. A 15-yr spinup run is carried out using the mean climate of the year 1979. The first 4-yr simulations are further discarded in the MAT-HI run since it is initialized with the soil moisture states in the nonirrigated condition. Therefore, the results from 1983 to 2007 are used for the analysis. For comparison, two additional simulations, H08-NAT and H08 (corresponding to MAT-NAT and MAT-HI simulations, respectively), are conducted using the H08 model (Table 1).

## 4. Model evaluation and analyses

This section presents the evaluation of model performance. To investigate the effect of model parameterizations (complexity) in the hydrological simulations, the modeled terrestrial water storage (TWS) is first compared with the observations from the Gravity Recovery and Climate Experiment (GRACE) satellite mission (Tapley et al. 2004). Then, river discharges of the MAT-NAT and MAT-HI simulations are evaluated against observed data from the Global Runoff Data Center (GRDC), and the effect of anthropogenic activities (reservoir operation and water withdrawal) on the river discharge is demonstrated over selected large river basins. Finally, simulated global irrigation water use is evaluated against the FAO estimates, and irrigation-induced changes on surface energy balance are briefly discussed.

### *a. Evaluation of the models against GRACE observations*

Figure 2 plots the terrestrial water storage anomaly (TWSA) comparison between GRACE observations and that from the MAT-NAT and H08-NAT simulations for nine selected large river basins located in different climatic regions. We compare MAT-NAT and H08-NAT simulations because the anthropogenic water regulation modules are identical in both models and the effects of reservoir storage are not significant in the selected basins. The 2002–07 monthly GRACE data used in this

study are from Chambers (2007) (version dpc200711, no smoothing). As seen in Fig. 2, for the semiarid and arid basins (e.g., Niger and Zambezi), MATSIRO captures the seasonal evolution of TWSA rather well, whereas H08 shows biased early and attenuated TWSA peaks. In these water-limited regions, TWS variation is mainly contributed by the variation of soil moisture, which is rather poorly simulated by the bucket model. In fact, bucket-type models tend to overestimate evapotranspiration because of the lack of any stomatal and surface resistances during low water stress periods (Chen et al. 1997; Koster and Milly 1997), implying that the bucket dries out too quickly, resulting in an overestimated buffer capacity before the rainy season starts. This issue is well known for the bucket model, which often behaves in an anomalous fashion compared with other LSMs (Chen et al. 1997; Desborough 1999). Furthermore, soil moisture variation is also attenuated because of the small constant capacity of the bucket (150 mm).

In water-abundant regions like the Amazon, Orinoco, and Ganges basins, no significant differences in TWSA are found between two models. In these regions, TWS fluctuations are mainly controlled by river storage, which also implicitly accounts for shallow groundwater storage variations (Kim et al. 2009), simulated by TRIP in both the models. In contrast, in snow-dominated basins (e.g., Ob and Yukon), two models exhibit considerable differences in TWSA because of the oversimplistic snow scheme used in H08 (Haddeland et al. 2011).

Based on the above results, it can be concluded that MATSIRO simulates soil moisture variation with better accuracy than the bucket-type model, particularly in semiarid regions. This result has important implications for simulated irrigation water requirements [Eq. (1)] because most irrigated areas are located in water-limited semiarid regions. Realistic simulation of soil moisture is the key to reliable estimation of irrigation water requirements.

### b. River discharge

Figure 3 presents the comparison of simulated river discharge for 30 large river basins against the observations provided by the GRDC. The basins are selected considering a wide coverage over different climatic regions and continents, and a good balance between the regulated and unregulated basins. If there are multiple gauging stations within a basin, the station with the largest catchment area or the longest observation data period is selected, except for some heavily regulated basins. In the heavily regulated river basins such as the Colorado, Missouri, and Snake, the station just downstream of the main reservoir is selected such that the effect of reservoir operation can be observed. It should be noted that the Missouri and Snake River basins are the tributaries of Mississippi and Columbia River basins, respectively. The upper-four rows in Fig. 3 present the comparison of river discharge of the basins with relatively less anthropogenic regulations. Simulated discharge agrees well with observations in the majority of these basins; seasonal hydrographs do not change notably after representing human regulations in the model because the total reservoir storage capacity (Sto.; see the numbers in each panel in Fig. 3) and consumptive water use from rivers are relatively small compared with the mean annual runoff volume. Differences in the simulated and observed timing of peak discharge are obvious in some river basins (e.g., Amazon, Ganges, and Yangtze), which is possibly due to the use of a globally constant flow velocity of 0.5 m $s^{-1}$. For the whole Amazon River basin, flow velocity of 0.5 m $s^{-1}$ is too fast, resulting in an early peak. On the contrary, for river basins like the Ganges, Yangtze, and Yukon, flow velocity of 0.5 m $s^{-1}$ is too slow, and results in the delayed peak discharge by about a month.

The lower-four rows in Fig. 3 depict the comparison of river discharge for some of the heavily regulated large river basins. In these basins, although the observed discharge is not perfectly captured by the model, considerable improvement is achieved in simulating the shape of the hydrograph after representing human regulations. Note that the annual water balance in the MAT-HI simulation is affected by water withdrawals upstream of the gauging station. In the Volga, Missouri, and Colorado River basins, reservoir simulation largely reduces the seasonal fluctuation of the hydrograph. Also in Vilyuy and Saguenay, in which the gauging stations are located just downstream of large reservoirs, consideration of reservoir operation significantly improves the seasonal cycle of river discharge.

Overall, the incorporation of anthropogenic water regulation modules significantly improves the simulation of low flow in most of the heavily regulated river basins. However, the peak is not largely reduced in some basins possibly because MATSIRO tends to overestimate runoff during high-flow season. Moreover, a generic operation rule is applied for all reservoirs, but in practice, the operation rules for individual reservoirs may vary greatly. Because such rules are not represented, the model targets the total annual release at the beginning of the operational year, which, in conjunction with the targeted monthly release, determines the total release for each month (Hanasaki et al. 2006). Furthermore, small reservoirs in the tributaries downstream of large reservoirs, which are not included in our database, may also have contributed to the underestimation of the effect of reservoirs on the simulated discharge in some basins.

### c. Irrigation water estimates

Simulated irrigation water requirements are compared with the estimates by FAO (FAO 2007) and a number of

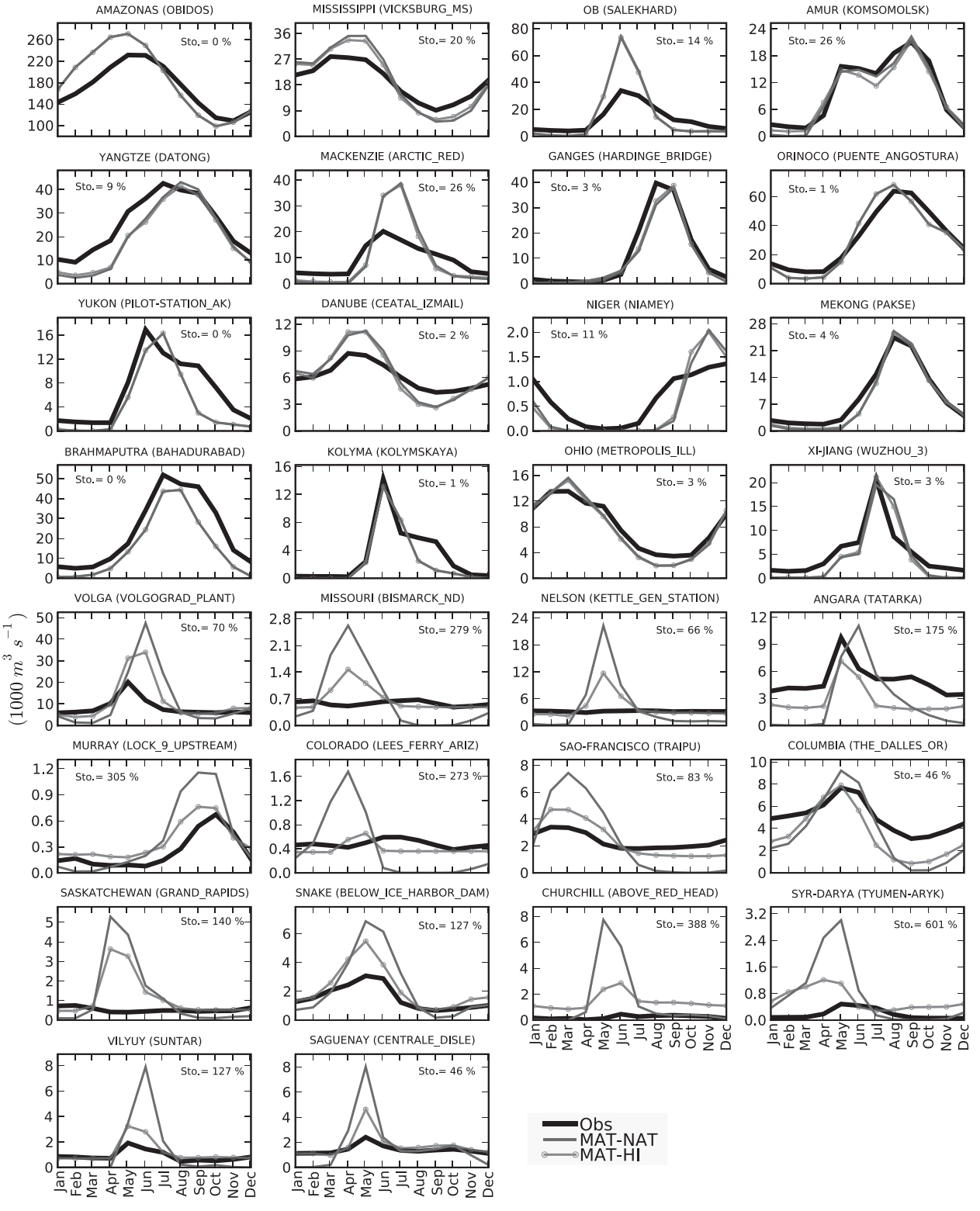


FIG. 3. Comparison of seasonal cycle of simulated river discharge (MAT-NAT and NAT-HI) against GRDC observations in 1000 $m^3$ $s^{-1}$. Seasonal cycle is calculated for the GRDC data availability period within 1983–2007. Numbers in each panel (i.e., Sto.) indicate the percentage of reservoir storage capacity upstream of the gauging station (shown in parenthesis) to observed mean annual runoff volume. Values less than 1 are shown as 0.

TABLE 2. Comparison of global irrigation water estimates ($km^3\ yr^{-1}$).

| Irrigation | This study* | | FAO | LPJmL | WaterGAP | H08 |
|---|---|---|---|---|---|---|
| (Year) | (1983–2007) | (2000) | (2000) | (1971–2000) | (2000) | (2000) |
| Demand | 906 ±62 | 1021 ±55 | — | 1364 | 1257 | 1598 |
| Withdrawal | 2158 ±134 | 2462 ±30 | 2660 | 2555 | 3256 | 3755 |

* Uncertainty ranges indicate ±1 standard deviation estimated from the results based on five precipitation datasets.

previous modeling studies. The FAO provides irrigation water withdrawal (gross irrigation requirement) but the model simulates potential irrigation water demand (net irrigation requirement). Therefore, the simulated potential irrigation water demand is converted into irrigation water withdrawal using the water use efficiency factor provided by Döll and Siebert (2002), which varies between 0.35 and 0.7, reflecting irrigation facilities and practices.

Table 2 presents a comparison of global irrigation water requirements. Note that in our simulation, water is assumed to be freely available at all times for consistency with previous studies. Results of the Water–Global Assessment and Prognosis (WaterGAP) and Lund–Potsdam–Jena managed land (LPJmL) models are obtained from Döll and Siebert (2002) and Rost et al. (2008), respectively. For the year 2000, simulated global irrigation water withdrawal of 2462 ±130 $km^3\ yr^{-1}$ compares well with the FAO estimates. The uncertainty range is estimated from the simulated irrigation withdrawal using different precipitation datasets (see section 2). H08 simulates a high irrigation demand, while the WaterGAP estimation is between with some overestimation in excess of FAO estimates. LPJmL results are averages for the period 1971–2000; a slightly higher estimate can be expected for the year 2000 because irrigated areas have significantly increased during this period. Our result indicates that the long-term mean withdrawal for the period 1983–2007 is ~12% smaller than that for the year 2000 (Table 2). The disparities among models can also be partly attributed to the differences in the irrigation efficiency used; for example, Rost et al. (2008) used a different efficiency data than that by the other studies compared here.

Because of the high uncertainties in global irrigation datasets (irrigated areas and irrigation water withdrawal) and differences in model parameterizations, comparison of irrigation estimates is not an easy task. Moreover, the documented estimates are not available for the same time period, making a direct comparison impossible. Nonetheless, the results of this study are in good agreement with the FAO estimates. As seen in Fig. 4a, country-level irrigation water withdrawals compare well with the estimates of FAO with a high $R^2$ of 0.952. Our model slightly underestimates irrigation water withdrawal mainly for countries using less irrigation water. However, this underestimation has little impact on the total global volume.

De Rosnay et al. (2003) estimated irrigation water for the Indian peninsula, which is a highly irrigated region, for the period 1987–1988 based on the ORCHIDEE LSM (Ducoudré et al. 1993). We compare our results for India with various previous estimates, including those of de Rosnay et al. (2003). As seen in Fig. 4b, there is a large variation in simulated irrigation water requirement among

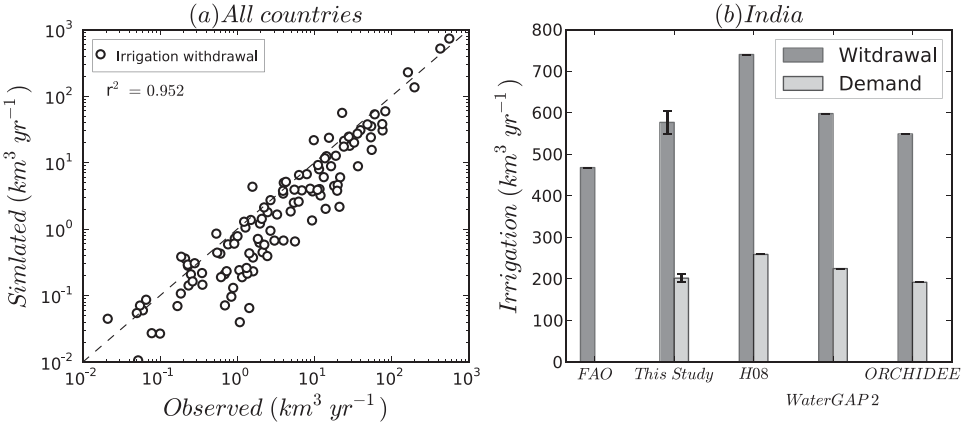


FIG. 4. (a) Country-based comparison of simulated irrigation water withdrawal with FAO estimates (FAO 2007). (b) Comparison for India only with various previous estimates for the year 1987 except for FAO (1983–87 averages) and ORCHIDEE (1987/88 averages). Error bars indicate ±1 standard deviation estimated from the results based on five precipitation datasets. Note that FAO provides only withdrawal data. All values are shown in $km^3\ yr^{-1}$.

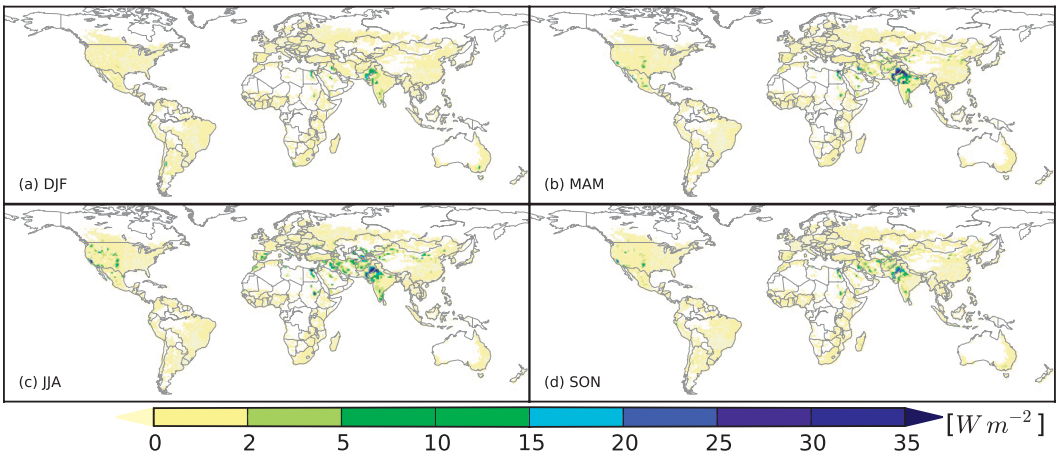


FIG. 5. Irrigation-induced changes in seasonal (DJF, MAM, JJA, and SON) latent heat flux (W $m^{-2}$) per grid cell averaged over the period 1983–2007. White color indicates grid cells with no irrigated croplands.

different models with the H08 model simulating the highest requirement; however, our result agrees well with the FAO estimates with slight overestimation. Even though the same forcing data and crop calendar are used, our results are significantly smaller compared with H08 results but closer to FAO estimates (Table 2, Fig. 4b). Therefore, the irrigation scheme developed in this study considerably improves the simulation of irrigation water requirements at both the global and regional scales compared to that by H08.

### *d. Effects of irrigation on energy balance components*

Increased soil water content through irrigation enhances evapotranspiration, which in turn transforms the surface energy balance. As shown in Fig. 5, latent heat flux (or evapotranspiration) increases significantly over the intensively irrigated regions such as northwestern India, Pakistan, the western United States, the Middle East, and the Nile Delta. The increase in the mean annual latent heat flux averaged over all irrigated grid cells is rather small (0.6 W $m^{-2}$; i.e., 1.2%). In general, the maximum increase in latent heat flux of up to 50 W $m^{-2}$ is observed during June–August (JJA) (Fig. 5)—the primary growing season in most irrigated areas in the Northern Hemisphere. In South Asia, particularly in western India and Pakistan, latent heat flux increase is large during both March–May (MAM) and JJA; during September–November (SON) and December–February (DJF), significant increase is not seen. In these regions, most precipitation occurs during the Indian monsoon season, which lasts for only a few months, with the rest of the year relatively dry. Climate is mostly semiarid, and evapotranspiration is largely governed by the availability of soil moisture. When water is abundantly supplied through irrigation, the wet soil and warm atmosphere over the cropland jointly result in large increase in latent heat flux. Averaged over the Indian subcontinent (5°–35°N and 65°–91°E), mean annual latent heat flux is increased by ~3.4 W $m^{-2}$, and this is in close agreement with 3.2 W $m^{-2}$ as estimated by de Rosnay et al. (2003) based on the irrigation scheme in the ORCHIDEE LSM. Haddeland et al. (2006a) estimated an increase in latent heat flux over the Colorado and Mekong River basins of 1.2 and 1.3 W $m^{-2}$, respectively—considerably larger than our estimates of 0.7 and 0.1 W $m^{-2}$. These differences can possibly be attributed to the difference in the precipitation, irrigated areas, and crop types data used among studies, which affect irrigation water requirement.

In the modestly irrigated areas in South America, Australia, Europe, and the southern part of Africa, irrigation causes only a small change in surface energy balance. In Southeast Asia and the eastern part of China, unlike the large change in the water balance, surface energy balance is not affected by irrigation, mainly because rice is the major crop and irrigation is served to sustain soil moisture at near-full saturation level during the growing season. Moreover, annual precipitation in these regions is relatively large and evapotranspiration is largely controlled by the availability of energy rather than soil moisture. Therefore, only a small percentage of irrigation is actually consumed by crops, with the remaining water discharging back to rivers as return flow. In addition, precipitation over standing water in the rice paddies causes an immediate increase in surface runoff.

Sensible heat flux and surface temperature decrease in response to the increase in latent heat flux. Decrease in mean annual surface temperature averaged over all irrigated grid cells is rather small (~0.04 K). Similar to latent heat flux, change in surface temperature is most pronounced during JJA with as high as −3.3 K in some highly irrigated grid cells in northwestern India, parts of

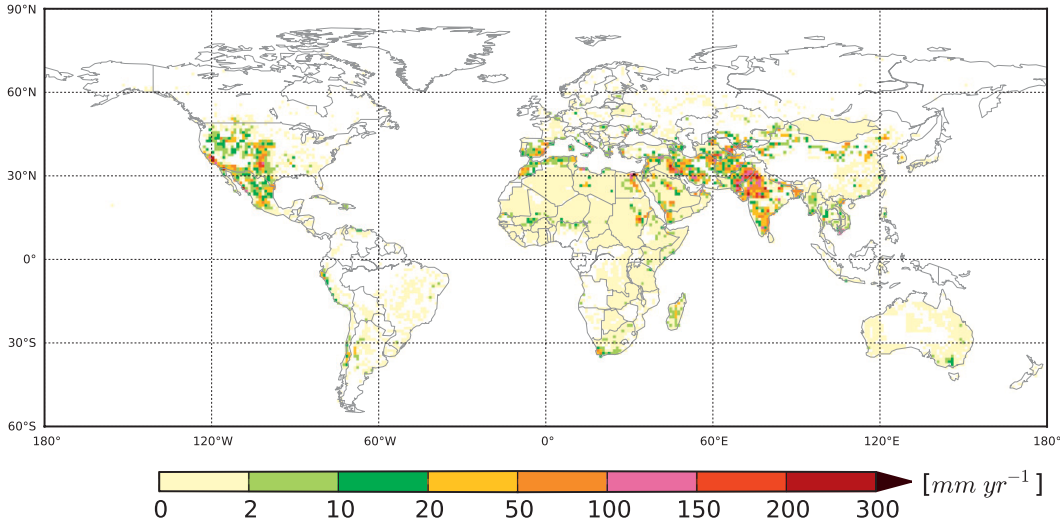


FIG. 6. Unsustainable anthropogenic water use or the NNBW for the year 2000 (mean of results based on five precipitation datasets; units are mm yr$^{-1}$).

Pakistan, the Nile Delta, and California's Central Valley. Such an alteration in the surface energy partitioning due to irrigation has significant implications on the global- and regional-scale water and energy balance studies (Boucher et al. 2004; Sacks et al. 2009; Puma and Cook 2010).

## 5. Model application: Estimation of unsustainable water use

In this section, we demonstrate the application of the integrated model to estimate the global unsustainable water use, which is the amount of water withdrawal exceeding local supplies (local runoff, storage in medium-sized reservoirs, and streamflow and reservoir release accumulated from upstream areas), usually termed the NNBW (Rost et al. 2008; Hanasaki et al. 2010). Figure 6 presents the simulated unsustainable water use for the year 2000. The total global volume is estimated as 454 $\pm$42 km$^3$ yr$^{-1}$, which is less than the estimates of Rost et al. (2008) (730 km$^3$ yr$^{-1}$) and Hanasaki et al. (2010) (703 km$^3$ yr$^{-1}$), but is within the range of 391 to 830 km$^3$ yr$^{-1}$ reported by Vörösmarty et al. (2005). The uncertainty range indicates $\pm$1 standard deviation estimated from the results based on different precipitation data. Recently, Siebert et al. (2010) estimated the global total groundwater use for irrigation to be ~545 km$^3$ yr$^{-1}$. Various other studies (e.g., Shah et al. 2000; Giordano 2009) have also reported the global total groundwater extractions within the range of 550–750 km$^3$ yr$^{-1}$. Because a part of the total extractions is assumed to be annually replenished, the unsustainable use in the range of 700 km$^3$ yr$^{-1}$ as reported by the previous modeling studies may not be realistic. Therefore, we consider that our model estimates the unsustainable water use with encouraging improvements over similar previous modeling studies.

As clearly seen in Fig. 6, large amounts of human water use in the Indian subcontinent, Middle East, Nile Delta, and western United States are unsustainable. However, we note that the groundwater processes such as recharge to the aquifers are not explicitly accounted in the model; and water is unlimitedly withdrawn when needed. Therefore, these results should be interpreted cautiously, particularly when comparing with fossil groundwater use, which might be smaller than our unsustainable use. In our model, return flows from irrigated areas discharge directly to rivers as surface or subsurface runoff. In reality, however, the return flows may recharge groundwater aquifers and respond more slowly to meteorological condition had the interactions between surface water and groundwater been considered in the model.

Recently, Wada et al. (2010, hereafter W2010) estimated 283 $\pm$40 km$^3$ yr$^{-1}$ of global groundwater depletion based on the national-scale data of groundwater extractions around the year 2000 and model-based groundwater recharge. However, their study was limited to semiarid and arid regions, and the countries where groundwater extraction data are not available were excluded. For example, our result shows ~16 km$^3$ yr$^{-1}$ of NNBW use in Afghanistan only, which was excluded in W2010. Therefore, it can be argued that W2010's results slightly underestimate global groundwater depletion. The spatial pattern varies greatly between our results and that of W2010 in some regions (e.g., eastern Pakistan, northeastern China, and Southeast Asia; see W2010, their Fig. 2).

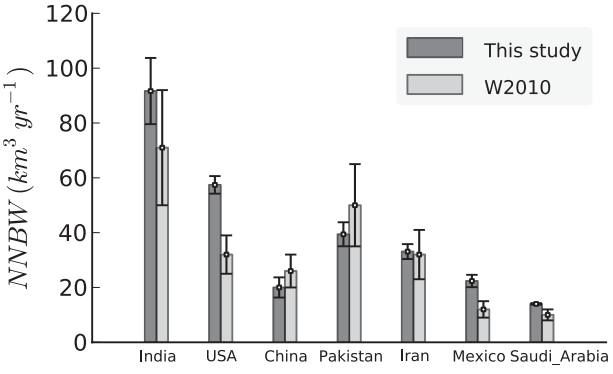


FIG. 7. Country-based comparison of unsustainable water use with W2010 for the year 2000 ($km^3\ yr^{-1}$). Error bars in W2010 represent the uncertainty in groundwater extraction data, and those in this study represent the uncertainty ($\pm 1$ standard deviation) caused by precipitation data.

In many countries in Southeast Asia, our results indicate significant unsustainable water use, which was nonexistent in the analysis of W2010.

Figure 7 presents a country-based comparison between simulated unsustainable water use and groundwater depletion of W2010 for selected countries with large unsustainable water use. As shown, the overestimation in our results mainly comes from India and the United States possibly because of the underestimation of the number of medium-sized reservoirs in the agricultural areas with less population distribution. Water stored in such reservoirs during wet seasons is utilized later when needed, contributing significantly to irrigation water supplies in many regions (Wisser et al. 2010b). For Pakistan, our results show lower unsustainable water use. However, without further investigation it is difficult to judge whether this discrepancy is due to the uncertainty of irrigated areas used in this study, or that the groundwater extraction data used by W2010 were relatively less reliable for Pakistan (Y. Wada 2011, personal communication). We also note that our estimate for Spain is possibly high (Fig. 6) because ~25% of water used for agriculture (Beltrán and Koo-Oshima 2006) is from desalinated seawater, which is not reflected in our model.

Our analysis indicates that for the total unsustainable water use, the contribution of domestic and industrial water is very small relative to agricultural water in all countries. Globally, ~95% of unsustainable water use is agricultural, which accounts for ~40% of total blue water used for irrigation. Throughout the simulation period of this study, unsustainable water use increased steadily from ~300 $km^3\ yr^{-1}$ during the early 1980s to ~450 $km^3\ yr^{-1}$ in 2000, peaked at ~470 $km^3\ yr^{-1}$ in 2003, and then steadily decreased during recent years. The decrease in recent years can be attributed to the increasing precipitation trend and relatively stable global temperature in the forcing data used, and is also due to the use of constant irrigated areas from 2003 to 2007.

## 6. Summary and conclusions

In this study, an integrated modeling framework for the assessment of anthropogenic impacts on the global terrestrial water cycle is developed by incorporating anthropogenic water regulation modules of a bucket-model-based GHM H08 into an advanced LSM MATSIRO. Further, a new irrigation scheme based on the soil moisture deficit is developed. Because MATSIRO was originally developed with a direct linkage to the parent GCM, the integrated model is applicable for both offline and online simulations at the global scale. In the present paper, the offline-simulation results are evaluated against available observational datasets. The effects of irrigation on surface energy balance are also briefly discussed. In addition, the model is applied to estimate unsustainable water use at the global scale.

Comparison of modeled TWSA with the GRACE satellite observations reveals that the MATSIRO outperforms H08, particularly in semiarid regions where TWSA is dominated by soil moisture variations. Simulated river discharge of the large river basins worldwide agrees well with the GRDC observations, and the incorporation of anthropogenic water regulation modules further improves simulations in the heavily regulated basins. Given that the integrated model is not directly tuned to reproduce observed river discharge and the development of reservoir operation module is still at its infancy, the results obtained from this study are encouraging.

Simulated irrigation water requirements also agree well with the documented national irrigation water use compared with the results of contemporary hydrological models. Using five different global precipitation datasets, ~5% uncertainty in the simulated global irrigation water withdrawal is estimated, but it can vary significantly from region to region depending on the reliability of precipitation data. In the extensively irrigated areas, irrigation significantly affects surface energy balance with the maximum increase of 50 W $m^{-2}$ in latent heat flux during JJA. However, the changes are rather small (~1.2%) when averaged annually and over global irrigated grid cells. It is noted that our results from an offline simulation should be interpreted with caution because they do not account for changes in climate forcing through feedback mechanisms. Extending the present study to further consider the feedbacks will be an important direction of future research.

By the application of the integrated model, the unsustainable anthropogenic water use (also called NNBW) is estimated. With a major improvement over the preceding

studies, our estimate of 454 ±42 $km^3$ $yr^{-1}$ compares fairly well with the documented global groundwater overdraft. The spatial pattern of unsustainable water use in our global simulation is similar to that of Wada et al. (2010) in most regions. Further, some regions in Southeast Asia using large amounts of unsustainable water but not considered in the analysis of Wada et al. (2010) can be seen in this study. Globally, NNBW supplies ~40% of total blue water used for irrigation around the year 2000.

There are still certain limitations in this study, including the lack of explicit representations of water table dynamics, water diversions, and evaporation from large reservoirs. Representation of the shallow water table in LSMs is critical because the fluxes near the water table significantly alter the vertical profile of soil moisture (Yeh and Eltahir 2005; Fan et al. 2007). At present, at least one-fourth of the world's population draws its water from aquifers (Jackson et al. 2001), and the exploitation of groundwater at unsustainable rates has resulted in rapid groundwater declines in many regions (Rodell et al. 2009). The next step, therefore, is to incorporate a groundwater representation (e.g., Yeh and Eltahir 2005; Niu et al. 2007) into our model. Such a modeling framework can be used to explicitly simulate groundwater withdrawal and recharge for a better estimation of unsustainable water use. In fact, the imaginary source in our MAT-HI simulation represents groundwater but it does not explicitly account for the groundwater processes such as recharge to the aquifers. For example, shallow aquifers may receive considerable amounts of recharge from irrigation return flows, and this important process has to be considered in estimating net water withdrawals.

Moreover, long-distance water diversions (e.g., the Colorado River aqueduct in the United States, Indira Gandhi canal in India, and Goldfields water supply scheme in Australia) may also have significant contributions in water supply to many water-limited regions. Because such processes are not yet represented in the model, our result may overestimate unsustainable water use in regions where most of the total water demand is met through water diversions. These issues have important implications for the global water resources assessments and have to be addressed in future research. Evaporation from large reservoirs may also have nonnegligible effects on regional water balance and this should also be accounted for in the model.

Despite these limitations, this study advances an important step beyond previous studies by providing a consistent modeling framework with a sophisticated LSM that accounts for important aspects of anthropogenic water use. In addition, the developed modeling framework can be coupled to its parent GCM to assess potential climate impacts and feedbacks due to anthropogenic disturbance of the terrestrial water cycle. The present integrated model is a useful tool for quantifying the contributions of various natural and anthropogenic factors controlling the variability of the hydrological cycle, and is, hence, also valuable for the projections of future water resources. To date, most climate model simulations used for the projection of future water resources do not explicitly account for the changes in land surface water and energy balance due to direct human intervention. This study contributes to advance the representation of anthropogenic water regulation activities within the framework of global climate models.

*Acknowledgments.* We wish to thank P. Döll and F. Portmann for providing global irrigation estimates of the WaterGAP model. We also thank the Global Runoff Data Center and GRACE science project for providing valuable datasets. We are also grateful to Y. Ishizaki for the support in model settings and S. Yoshikawa for helping with data preparation. The first author acknowledges the support by the Ministry of Education, Culture, Sports, Science and Technology (MEXT). This work was partially supported by Global Environment Research Fund (GERF; S5) from the Ministry of Environment, JSPS KAKENHI, Grants-in-Aid for Scientific Research (S)(23226012), and Innovative Program of Climate Change Projection for the 21st Century from MEXT. We also thank three anonymous reviewers for the constructive comments that improved the manuscript.

## REFERENCES

Adler, R. F., and Coauthors, 2003: The version-2 Global Precipitation Climatology Project (GPCP) monthly precipitation analysis (1979–present). *J. Hydrometeor.,* **4,** 1147–1167.

Alcamo, J., P. Döll, T. Henrichs, F. Kaspar, B. Lehner, T. Rösch, and S. Siebert, 2003: Development and testing of the WaterGAP 2 global model of water use and availability. *Hydrol. Sci. J.,* **48,** 317–337.

Allen, R. G., L. S. Pereira, D. Raes, and M. Smith, 1998: Crop evapotranspiration—Guidelines for computing crop water requirements. FAO Irrigation and Drainage Paper 56, 300 pp.

Beltrán, J., and S. Koo-Oshima, 2006: Water desalination for agricultural applications. FAO Land and Water Discussion Paper 5, 48 pp.

Beven, K. J., and M. J. Kirkby, 1979: A physically based, variable contributing area model of basin hydrology. *Hydrol. Sci. Bull.,* **24,** 43–69.

Boucher, O., G. Myhre, and A. Myhre, 2004: Direct human influence of irrigation on atmospheric water vapour and climate. *Climate Dyn.,* **22,** 597–603.

Cai, X., and M. W. Rosegrant, 2002: Global water demand and supply projections, Part 1: A modeling approach. *Water Int.,* **27,** 159–169.

Chambers, D. P., 2007: Converting Release-04 gravity coefficients into maps of equivalent water thickness. Jet Propulsion Laboratory Tech. Rep., 9 pp. [Available online at http://grace.jpl.nasa.gov/files/GRACE-dpc200711_RL04.pdf.]

Chen, M., P. Xie, J. E. Janowiak, and P. A. Arkin, 2002: Global land precipitation: A 50-yr monthly analysis based on gauge observations. *J. Hydrometeor.,* **3,** 249–266.

——, W. Shi, P. Xie, V. B. S. Silva, V. E. Kousky, R. W. Higgins, and J. E. Janowiak, 2008: Assessing objective techniques for gauge-based analyses of global daily precipitation. *J. Geophys. Res.,* **113,** D04110, doi:10.1029/2007JD009132.

Chen, T. H., and Coauthors, 1997: Cabauw experimental results from the project for intercomparison of land-surface parameterization schemes. *J. Climate,* **10,** 1194–1215.

Collatz, G., J. T. Ball, C. Grivet, and J. A. Berry, 1991: Physiological and environmental regulation of stomatal conductance, photosynthesis and transpiration: A model that includes a laminar boundary layer. *Agric. For. Meteor.,* **54,** 107–136.

Cśaki, C., and C. de Haan, 2003: *Reaching the Rural Poor: A Renewed Strategy for Rural Development*. World Bank Publications, 204 pp.

Decharme, B., R. Alkama, H. Douville, M. Becker, and A. Cazenave, 2010: Global evaluation of the ISBA-TRIP continental hydrological system. Part II: Uncertainties in river routing simulation related to flow velocity and groundwater storage. *J. Hydrometeor.,* **11,** 601–617.

Desborough, C., 1999: Surface energy balance complexity in GCM land surface models. *Climate Dyn.,* **15,** 389–403.

de Rosnay, P., J. Polcher, K. Laval, and M. Sabre, 2003: Integrated parameterization of irrigation in the land surface model ORCHIDEE. Validation over Indian Peninsula. *Geophys. Res. Lett.,* **30,** 1986, doi:10.1029/2003GL018024.

Dirmeyer, P. A., X. Gao, M. Zhao, Z. Guo, T. Oki, and N. Hanasaki, 2006: GSWP-2: Multimodel analysis and implications for our perception of the land surface. *Bull. Amer. Meteor. Soc.,* **87,** 1381–1397.

Döll, P., and S. Siebert, 2002: Global modeling of irrigation water requirements. *Water Resour. Res.,* **38,** 1037, doi:10.1029/2001WR000355.

——, K. Fiedler, and J. Zhang, 2009: Global-scale analysis of river flow alterations due to water withdrawals and reservoirs. *Hydrol. Earth Syst. Sci.,* **13,** 2413–2432.

Ducoudré, N. I., K. Laval, and A. Perrier, 1993: SECHIBA, a new set of parameterizations of the hydrologic exchanges at the land–atmosphere interface within the LMD atmospheric general circulation model. *J. Climate,* **6,** 248–273.

Fan, Y., G. Miguez-Macho, C. P. Weaver, R. Walko, and A. Robock, 2007: Incorporating water table dynamics in climate modeling: 1. Water table observations and equilibrium water table simulations. *J. Geophys. Res.,* **112,** D10125, doi:10.1029/2006JD008111.

FAO, cited 2007: AQUASTAT. [Available online at http://www.fao.org/nr/water/aquastat/main/index.stm.]

Freydank, K., and S. Siebert, 2008: Towards mapping the extent of irrigation in the last century: Time series of irrigated area per country. Frankfurt Hydrology Paper-08, 46 pp.

Giordano, M., 2009: Global groundwater? Issues and solutions. *Annu. Rev. Environ. Resour.,* **34,** 153–178.

Haddeland, I., D. P. Lettenmaier, and T. Skaugen, 2006a: Effects of irrigation on the water and energy balances of the Colorado and Mekong river basins. *J. Hydrol.,* **324,** 210–223.

——, T. Skaugen, and D. P. Lettenmaier, 2006b: Anthropogenic impacts on continental surface water fluxes. *Geophys. Res. Lett.,* **33,** L08406, doi:10.1029/2006GL026047.

——, and Coauthors, 2011: Multimodel estimate of the global terrestrial water balance: Setup and first results. *J. Hydrometeor.,* **12,** 869–884.

Hanasaki, N., S. Kanae, and T. Oki, 2006: A reservoir operation scheme for global river routing models. *J. Hydrol.,* **327,** 22–41.

——, ——, ——, K. Masuda, K. Motoya, N. Shirakawa, Y. Shen, and K. Tanaka, 2008a: An integrated model for the assessment of global water resources—Part 1: Model description and input meteorological forcing. *Hydrol. Earth Syst. Sci.,* **12,** 1007–1025.

——, ——, ——, ——, ——, ——, ——, and ——, 2008b: An integrated model for the assessment of global water resources—Part 2: Applications and assessments. *Hydrol. Earth Syst. Sci.,* **12,** 1027–1037.

——, T. Inuzuka, S. Kanae, and T. Oki, 2010: An estimation of global virtual water flow and sources of water withdrawal for major crops and livestock products using a global hydrological model. *J. Hydrol.,* **384,** 232–244.

Hasumi, H., and S. Emori, Eds., 2004: K-1 coupled model (MIROC) description. K-1 Tech. Rep. 1, 34 pp. [Available online at http://www.ccsr.u-tokyo.ac.jp/~agcmadm/.]

Helkowski, J. H., 2004: Global patterns of soil moisture and runoff: An assessment of water availability. M.S. thesis, University of Wisconsin—Madison, 51 pp.

Hirabayashi, Y., S. Kanae, I. Struthers, and T. Oki, 2005: A 100-year (1901–2000) global retrospective estimation of the terrestrial water cycle. *J. Geophys. Res.,* **110,** D19101, doi:10.1029/2004JD005492.

ICOLD, 1998: *World Register of Dams*. International Commission on Large Dams.

——, 2003: *World Register of Dams*. International Commission on Large Dams.

Jackson, R., S. Carpenter, C. Dahm, D. McKnight, R. Naiman, S. Postel, and S. Running, 2001: Water in a changing world. *Ecol. Appl.,* **11,** 1027–1045.

Kim, H., P. J.-F. Yeh, T. Oki, and S. Kanae, 2009: Role of rivers in the seasonal variations of terrestrial water storage over global basins. *Geophys. Res. Lett.,* **36,** L17402, doi:10.1029/2009GL039006.

Koster, R. D., and P. C. D. Milly, 1997: The interplay between transpiration and runoff formulations in land surface schemes used with atmospheric models. *J. Climate,* **10,** 1578–1591.

——, and Coauthors, 2004: Regions of strong coupling between soil moisture and precipitation. *Science,* **305,** 1138–1140.

Krysanova, V., D.-I. Müller-Wohlfeil, and A. Becker, 1998: Development and test of a spatially distributed hydrological/water quality model for mesoscale watersheds. *Ecol. Modell.,* **106,** 261–289.

Leff, B., N. Ramankutty, and J. A. Foley, 2004: Geographic distribution of major crops across the world. *Global Biogeochem. Cycles,* **18,** GB1009, doi:10.1029/2003GB002108.

Lobell, D., G. Bala, A. Mirin, T. Phillips, R. Maxwell, and D. Rotman, 2009: Regional differences in the influence of irrigation on climate. *J. Climate,* **22,** 2248–2255.

Manabe, S., 1969: Climate and ocean circulation: I. The atmospheric circulation and the hydrology of the earth's surface. *Mon. Wea. Rev.,* **97,** 739–774.

Ngo-Duc, T., J. Polcher, and K. Laval, 2005: A 53-year forcing data set for land surface models. *J. Geophys. Res.,* **110,** D06116, doi:10.1029/2004JD005434.

Nilsson, C., C. A. Reidy, M. Dynesius, and C. Revenga, 2005: Fragmentation and flow regulation of the world's large river systems. *Science,* **308,** 405–408.

Niu, G.-Y., Z.-L. Yang, R. E. Dickinson, L. E. Gulden, and H. Su, 2007: Development of a simple groundwater model for use in climate models and evaluation with Gravity Recovery and Climate Experiment data. *J. Geophys. Res.,* **112,** D07103, doi:10.1029/2006JD007522.

Oki, T., and Y. C. Sud, 1998: Design of Total Runoff Integrating Pathways (TRIP)—A global river channel network. *Earth Interact.,* **2,** 1–37.

——, and S. Kanae, 2006: Global hydrological cycles and world water resources. *Science,* **313,** 1068–1072.

——, T. Nishimura, and P. Dirmeyer, 1999: Assessment of annual runoff from land surface models using Total Runoff Integrating Pathways (TRIP). *J. Meteor. Soc. Japan,* **77,** 235–255.

Onogi, K., and Coauthors, 2007: The JRA-25 Reanalysis. *J. Meteor. Soc. Japan,* **85,** 369–432.

Ozdogan, M., M. Rodell, H. K. Beaudoing, and D. L. Toll, 2010: Simulating the effects of irrigation over the United States in a land surface model based on satellite-derived agricultural data. *J. Hydrometeor.,* **11,** 171–184.

Puma, M. J., and B. I. Cook, 2010: Effects of irrigation on global climate during the 20th century. *J. Geophys. Res.,* **115,** D16120, doi:10.1029/2010JD014122.

Ramankutty, N., and J. A. Foley, 1999: Estimating historical changes in global land cover: Croplands from 1700 to 1992. *Global Biogeochem. Cycles,* **13,** 997–1027.

Robock, A., K. Vinnikov, C. Schlosser, N. Speranskaya, and Y. Xue, 1995: Use of midlatitude soil moisture and meteorological observations to validate soil moisture simulations with biosphere and bucket models. *J. Climate,* **8,** 15–35.

Rodell, M., I. Velicogna, and J. S. Famiglietti, 2009: Satellite-based estimates of groundwater depletion in India. *Nature,* **460,** 999–1002.

Rost, S., D. Gerten, A. Bondeau, W. Lucht, J. Rohwer, and S. Schaphoff, 2008: Agricultural green and blue water consumption and its influence on the global water system. *Water Resour. Res.,* **44,** W09405, doi:10.1029/2007WR006331.

Rudolf, B., and U. Schneider, 2005: Calculation of gridded precipitation data for the global land-surface using in-situ gauge observations. *Proc. Second Workshop of the Int. Precipitation Working Group,* Monterey, CA, IPWG, 231–247.

Sacks, W. J., B. I. Cook, N. Buenning, S. Levis, and J. H. Helkowski, 2009: Effects of global irrigation on the near-surface climate. *Climate Dyn.,* **33,** 159–175.

Sellers, P. J., and Coauthors, 1997: Modeling the exchanges of energy, water, and carbon between continents and the atmosphere. *Science,* **275,** 502–509.

Shah, T., D. Molden, R. Sakthivadivel, and D. Seckler, 2000: The global groundwater situation: Overview of opportunities and challenges. International Water Management Institute Rep., 21 pp.

Shiklomanov, I. A., 2000: Appraisal and assessment of world water resources. *Water Int.,* **25,** 11–32.

——, and J. C. Rodda, Eds., 2003: *World Water Resources at the Beginning of the 21st Century*. International Hydrology Series, Cambridge University Press, 435 pp.

Shukla, J., and Y. Mintz, 1982: Influence of land-surface evapotranspiration on the Earth's climate. *Science,* **215,** 1498–1501.

Siebert, S., P. Döll, S. Feick, J. Hoogeveen, and K. Frenken, cited 2007: Global Map of Irrigation Areas version 4.0.1. [Available online at http://www.fao.org/nr/water/aquastat/irrigationmap/index10.stm.]

——, J. Burke, J. M. Faures, K. Frenken, J. Hoogeveen, P. Döll, and F. T. Portmann, 2010: Groundwater use for irrigation—A global inventory. *Hydrol. Earth Syst. Sci.,* **14,** 1863–1880.

Stieglitz, M., D. Rind, J. Famiglietti, and C. Rosenzweig, 1997: An efficient approach to modeling the topographic control of surface hydrology for regional and global climate modeling. *J. Climate,* **10,** 118–137.

Takata, K., S. Emori, and T. Watanabe, 2003: Development of the minimal advanced treatments of surface interaction and runoff. *Global Planet. Change,* **38,** 209–222.

Tang, Q., T. Oki, S. Kanae, and H. Hu, 2007: The influence of precipitation variability and partial irrigation within grid cells on a hydrological simulation. *J. Hydrometeor.,* **8,** 499–512.

Tapley, B. D., S. Bettadpur, J. C. Ries, P. F. Thompson, and M. M. Watkins, 2004: GRACE measurements of mass variability in the Earth system. *Science,* **305,** 503–505.

Vörösmarty, C. J., and D. Sahagian, 2000: Anthropogenic disturbance of the terrestrial water cycle. *Bioscience,* **50,** 753–765.

——, P. Green, J. Salisbury, and R. B. Lammers, 2000: Global water resources: Vulnerability from climate change and population growth. *Science,* **289,** 284–288.

——, C. Lévêque, and C. Revenga, 2005: Fresh water. *Ecosystems and Human Well-Being: Current State and Trends,* R. M. Hassan, R. Scholes, and N. Ash, Eds., Millennium Ecosystem Assessment Series, Vol. 1, Island Press, 165–208.

——, and Coauthors, 2010: Global threats to human water security and river biodiversity. *Nature,* **467,** 555–561.

Wada, Y., L. P. H. van Beek, C. M. van Kempen, J. W. T. M. Reckman, S. Vasak, and M. F. P. Bierkens, 2010: Global depletion of groundwater resources. *Geophys. Res. Lett.,* **37,** L20402, doi:10.1029/2010GL044571.

Watanabe, T., 1994: Bulk parameterization for a vegetated surface and its application to a simulation of nocturnal drainage flow. *Bound.-Layer Meteor.,* **70,** 13–35.

Wisser, D., B. M. Fekete, C. J. Vörösmarty, and A. H. Schumann, 2010a: Reconstructing 20th century global hydrography: A contribution to the Global Terrestrial Network—Hydrology (GTN-H). *Hydrol. Earth Syst. Sci.,* **14,** 1–24.

——, S. Frolking, E. M. Douglas, B. M. Fekete, A. H. Schumann, and C. J. Vörösmarty, 2010b: The significance of local water resources captured in small reservoirs for crop production—A global-scale analysis. *J. Hydrol.,* **384,** 264–275.

Xie, P., and P. A. Arkin, 1997: Global precipitation: A 17-year monthly analysis based on gauge observations, satellite estimates, and numerical model outputs. *Bull. Amer. Meteor. Soc.,* **78,** 2539–2558.

Yeh, P. J.-F., and E. A. B. Eltahir, 2005: Representation of water table dynamics in a land surface scheme. Part I: Model development. *J. Climate,* **18,** 1861–1880.